XLVI CILAMCE
VITÓRIA - ES - BRAZIL - 2025
XLVI IBERO-LATIN AMERICAN CONGRESS ON COMPUTATIONAL METHODS IN ENGENEERING

Direct Interpolation-Based Matrix Assembly in the Boundary Element Method for Elasticity

L. S. Campos[1], C. F. Loeffler[1]

[1]*Department of Mechanical Engineering, UFES*
Avenida Fernando Ferrari, 514, 29060-410, Vitória/ES, Brazil
lucas.s.campos@ufes.br, carlos.loeffler@ufes.br

Abstract.

A strategy for faster matrix assembly in the Boundary Element Method (BEM) is applied to elasticity problems in this work. The key idea lies in extending the direct interpolation method, conventionally applied to domain integrals, to boundary integrals. This approach yields enhanced computational efficiency while preserving solution accuracy and ensuring convergence with mesh refinement. The effectiveness of this technique is demonstrated through its application to two-dimensional elasticity problems.

Keywords: Boundary Element Method, Direct Interpolation Method, Linear Elasticity

1 Introduction

The Boundary Element Method (BEM) is a numerical approaches that different from the Finite Element Method (FEM) and the Finite Difference Method (FDM), BEM reformulates the governing PDEs into integral equations that are applied solely over the boundary of the problem domain [1].

Despite the compelling advantages offered by its boundary-only formulation, conventional BEM encounters significant computational hurdles, particularly when applied to large-scale engineering problems. A fundamental aspect of BEM is that the interactions between boundary elements are non-local. This is a direct consequence of the nature of Green's functions, which represent the influence of a point source across the entire domain. Consequently, every boundary element interacts with every other element, leading to the formation of dense matrices. The very feature that provides BEM its advantage of reduced dimensionality simultaneously introduces its most significant computational burden. Both the memory required for their storage and the computational time necessary for performing matrix-vector products scale quadratically with the number of degrees of freedom. Moreover, when direct solvers are employed to solve these systems of linear equations, the computational time scales cubically. These scaling characteristics present substantial hurdles for the application of BEM to large-scale problems.

The Fast Multipole Method (FMM) and Hierarchical Matrices (H-Matrices)[2–5] are the most well-known acceleration strategies of BEM. They reduce the order of complextity to linear overcoming these limitations and elevating BEM from a elegant but computationally impractical method to a competitive tool for complex, large-scale problems.

Direct interpolation methods within the Boundary Element Method(DIBEM)[6–8] have been primarily employed to transform domain integrals into equivalent boundary integrals. This application is particularly crucial for problems that involve non-homogeneous materials, distributed body forces, or non-linearities. These factors traditionally introduce volume integrals into the BEM formulation, which, if not addressed, would necessitate full domain discretization. Such discretization would negate one of BEM's most significant advantages.

The present work introduces a strategy that extends the application of DIBEM. This paper applies it directly to accelerate the assembly of the primary BEM matrices for elasticity, which arise from boundary integrals. This approach has proved itself successful for potential problems in [9] and is extended here. This technique retains the order of complexity however it can be easily extended to be used together with H-matrices. The effectiveness of this novel technique will be demonstrated through its application to two-dimensional elasticity problems.

2 Governing equations

In accordance with the established BEM mathematical procedures delineated in [10], the integral boundary equation for linear elasticity can be written as:

$$C_{ij}(x_d)u_j(x_d) = \int_\Gamma u_j T^*_{ij} d\Gamma - \int_\Gamma U^*_{ij} t_j \Gamma, \tag{1}$$

where $C_{ij}(x_d)$ denotes the jump tensor, with x_d representing a point on the boundary Γ. Notably, for a smooth point on the boundary, $C_{ij}(x_d)$ assumes the value of $0.5\delta_{ij}$, where δ_{ij} is the Kronecker delta. Additionally, U^*_{ij} and T^*_{ij} correspond to the fundamental solutions for displacements and tractions, respectively, derived from Kelvin's solution for an infinite elastic medium. The terms u_j and t_j represent the boundary displacements and tractions, respectively.

2.1 Division of the Boundary into Elements

The boundary Γ is discretized into n discontinuous isoparametric elements, Γ_e, such that $\Gamma = \sum_1^n \Gamma_e$. The integral boundary equation can then be expressed as a sum over these elements:

$$C_{ij}(x_d)u_j(x_d) = \sum_{e=1}^{n} \int_{\Gamma_e} u_j T^*_{ij} d\Gamma_e - \sum_{e=1}^{n} \int_{\Gamma_e} U^*_{ij} t_j d\Gamma_e \tag{2}$$

The geometry, the displacements and the tractions must be defined over each element. What sets this approach apart is the interpolation of the entire integrand, a departure from classical BEM that only interpolate the variables themselves, a technique that was initially introduced for domain integrals in DIBEM. The interpolation scheme is written for m nodes and their corresponding N_i shape functions is expressed as:

$$U^*_{ij} t_j \quad = \sum_{k=1}^{m} N_k(\xi)(U^*_{ij} t_j)^{(k)} \tag{3}$$

$$u_j T^*_{ij} \quad = \sum_{k=1}^{m} N_k(\xi)(u_j T^*_{ij})^{(k)} \tag{4}$$

In these equations, the superscript $^{(k)}$ denotes the value of the enclosed term evaluated at node k.

The interpolated values from Equation (3) are then substituted into Equation (2), yielding:

$$C_{ij}(x_d)u_j(x_d) = \sum_{e=1}^{n} \int_{\Gamma_e} \sum_{k=1}^{m} N_k(\xi)(u_j T^*_{ij})^{(k)} d\Gamma_e - \sum_{e=1}^{n} \int_{\Gamma_e} \sum_{k=1}^{m} N_k(\xi)(U^*_{ij} t_j)^{(k)} d\Gamma_e \tag{5}$$

As only the shape functions vary along the element, the equation can be rewritten as:

$$C_{ij}(x_d)u_j(x_d) = \sum_{e=1}^{n} \int_{\Gamma_e} \sum_{k=1}^{m} N_k(\xi) d\Gamma_e (u_j T^*_{ij})^{(k)} - \sum_{e=1}^{n} \int_{\Gamma_e} \sum_{k=1}^{m} N_k(\xi) d\Gamma_e (U^*_{ij} t_j)^{(k)} \tag{6}$$

Defining I_i as $\int N_i d\Gamma$, considering the global index of each node and all the source points yields a system of $2nm$ linear algebraic equations that can be writen in matrix form as:

$$\begin{bmatrix} I_1 T^{*\,(1)}_{11} - C^{(1)}_{11} & I_1 T^{*\,(1)}_{12} - C^{(1)}_{12} & \cdots & I_{nm} T^{*\,(nm)}_{11} & I_{nm} T^{*\,(nm)}_{12} \\ I_1 T^{*\,(1)}_{21} - C^{(1)}_{21} & I_1 T^{*\,(1)}_{22} - C^{(1)}_{22} & \cdots & I_{nm} T^{*\,(nm)}_{21} & I_{nm} T^{*\,(nm)}_{22} \\ & \vdots & \ddots & \vdots & \\ I_1 T^{*\,(1)}_{11} - C^{(1)}_{11} & I_1 T^{*\,(1)}_{12} - C^{(1)}_{12} & \cdots & I_{nm} T^{*\,(nm)}_{11} & I_{nm} T^{*\,(nm)}_{12} \\ I_1 T^{*\,(1)}_{21} - C^{(1)}_{21} & I_1 T^{*\,(1)}_{22} - C^{(1)}_{22} & \cdots & I_{nm} T^{*\,(nm)}_{21} & I_{nm} T^{*\,(nm)}_{22} \end{bmatrix} \begin{bmatrix} u^{(1)}_1 \\ u^{(1)}_2 \\ \vdots \\ u^{(nm)}_1 \\ u^{(nm)}_2 \end{bmatrix} =$$

$$\begin{bmatrix} I_1 U^{*\,(1)}_{11} - C^{(1)}_{11} & I_1 U^{*\,(1)}_{12} - C^{(1)}_{12} & \cdots & I_{nm} U^{*\,(nm)}_{11} & I_{nm} U^{*\,(nm)}_{12} \\ I_1 U^{*\,(1)}_{21} - C^{(1)}_{21} & I_1 U^{*\,(1)}_{22} - C^{(1)}_{22} & \cdots & I_{nm} U^{*\,(nm)}_{21} & I_{nm} U^{*\,(nm)}_{22} \\ & \vdots & \ddots & \vdots & \\ I_1 U^{*\,(1)}_{11} - C^{(1)}_{11} & I_1 U^{*\,(1)}_{12} - C^{(1)}_{12} & \cdots & I_{nm} U^{*\,(nm)}_{11} & I_{nm} U^{*\,(nm)}_{12} \\ I_1 U^{*\,(1)}_{21} - C^{(1)}_{21} & I_1 U^{*\,(1)}_{22} - C^{(1)}_{22} & \cdots & I_{nm} U^{*\,(nm)}_{21} & I_{nm} U^{*\,(nm)}_{22} \end{bmatrix} \begin{bmatrix} t^{(1)}_1 \\ t^{(1)}_2 \\ \vdots \\ t^{(nm)}_1 \\ t^{(nm)}_2 \end{bmatrix}, \tag{7}$$

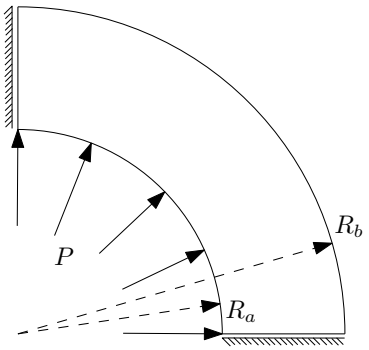


Figure 1. Geometry of the cylinder.

which are arranged in matrix form as:

$$Hu = Gt \tag{8}$$

When the element's distance to the source point is smaller than two times its length, the direct interpolation begins to behave poorly. This behaviour was observed in [9] for potential problems but for elastic problems this issue is more prominent as the singularities here are more severe. To circumvent this issue, these terms are calculated in the classical manner where the fundamental solution is not interpolated and only the field variables are. The nearly-singular and weakly-singular terms are dealt with by the sinh transformation [11], and the strongly-singular term is calculated indirectly by considering rigid body motion.

3 Numerical examples

In this study, the performance of DIBEM is assessed against traditional BEM using three distinct examples. Quadratic discontinuous elements are employed for all simulations. The error is quantified by the relative mean error, calculated at one hundred uniformly distributed internal points.

3.1 Pressurized cylinder

In Figure 1, the geometry and boundary conditions is shown for this problem. Geometric and material properties are shown in Table 1.

Table 1. Geometric and material properties for the pressurized cylinder.

Property	**Symbol**	**Value**
Inner Radius	R_a	50 mm
Outer Radius	R_b	100 mm
Young's Modulus	E	200 GPa
Poisson's ratio	ν	0.32
Pressure	P	100 N/mm

The analytical solution is given by:

$$\begin{aligned} u_r &= \frac{(1+v)PR_a^2}{(R_b^2 - R_a^2)\,E}\left[(1-2v)r + \frac{R_b^2}{r}\right] \\ \sigma_r &= \frac{a^2 P}{b^2 - a^2}\left(1 - \frac{b^2}{r^2}\right) \\ \sigma_\theta &= \frac{a^2 P}{b^2 - a^2}\left(1 + \frac{b^2}{r^2}\right) \end{aligned} \tag{9}$$

In the given problem, the DIBEM exhibited a slightly better performance across all discretizations when compared to BEM as depicted in Figure 2.

Table 2. Material properties and applied load for the cantilever beam

Property	**Symbol**	**Value**
Length	L	48
Depth	D	12
Young's Modulus	E	3×10^7
Poisson's ratio	v	0.3
Distributed load	P	1000

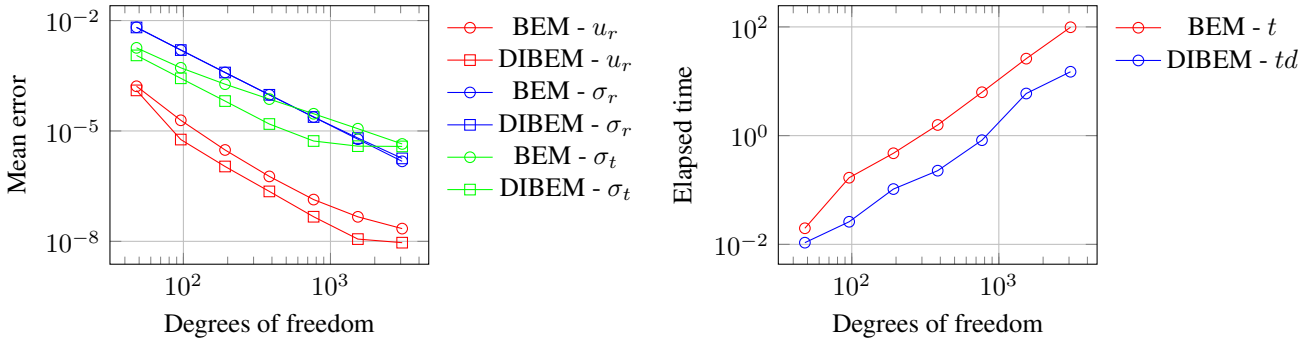


Figure 2. Mean errors and elapsed time for the Pressurized cylinder

One of the benefits of employing the proposed method is its computational efficiency. The fundamental solution in DIBEM requires computation solely at every combination of source points, which contrasts with the traditional BEM, where the fundamental solution has to be evaluated at every integration point for each distinct source point, which significantly increases the computational effort required as can be observed in figure 2. Using DIBEM resulted in a computational speed-up of approximately 10 times.

3.2 Cantilever beam

This example consists on a cantilever beam of dimensions $L \times D$ and unit depth, analysed under a plane stress assumption. As shown in Figure 3, its boundary conditions include a parabolic traction applied at the beam's end, which is described by:

$$t_2(y) = -\frac{P}{2I}\left(\frac{D^2}{4} - y^2\right) \tag{10}$$

where $I = D^3/12$ is the moment of inertia.

Analytical solutions for displacements and σ_{xx} are:

$$\begin{aligned} u_1(x,y) &= -\frac{Py}{6EI}\left[(6L-3x)x + (2+v)\left(y^2 - \frac{D^2}{4}\right)\right] \\ u_2(x,y) &= \frac{P}{6EI}\left[(3v)y^2(L-x) + (4+5v)\frac{D^2 x}{4} + (3L-x)x^2\right] \\ \sigma_{xx}(x,y) &= -\frac{P(L-x)y}{I} \end{aligned} \tag{11}$$

Geometric and material properties are shown in Table 3.

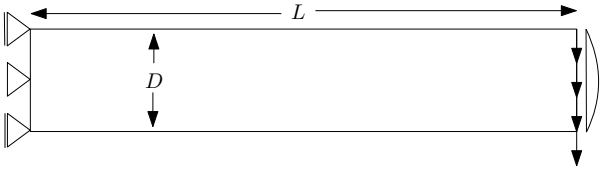


Figure 3. Geometry a cantilever beam in bending.

Table 3. Material properties and applied load for the cantilever beam

Property	Symbol	Value
Length	L	48
Depth	D	12
Young's Modulus	E	3×10^7
Poisson's ratio	v	0.3
Distributed load	P	1000

As depicted in Figure 4, DIBEM and BEM demonstrated very similar performance across all discretizations in this problem. However, for the most discretized case, DIBEM showed a small advantage with slightly smaller errors. Consistent with previous example, a speed-up of approximately 10 in elapsed time was noted.

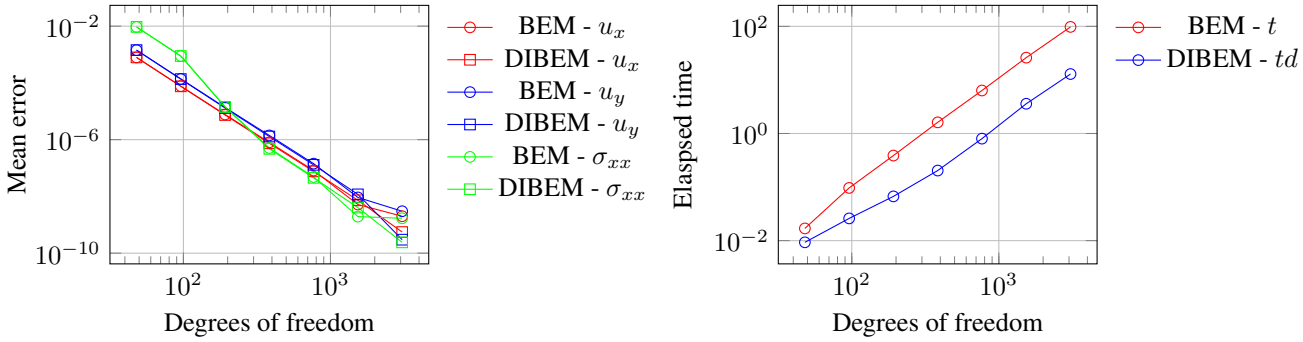


Figure 4. Mean errors and elapsed time for the cantilever beam

4 Conclusion

In this paper, we investigated the capabilities of the proposed DIBEM formulation for elasticity problems. Our preliminary findings reveal that DIBEM achieves a comparable precision to traditional methods while simultaneously offering a substantial performance improvement, marked by an approximate 10-fold speedup. Using two times the element length to This underscores DIBEM's versatility and indicates its potential for simulating more complex scenarios.

References

[1] J. T. Katsikadelis. *The Boundary Element Method for Engineers and Scientists*. Elsevier, Academic Press, 2016.

[2] E. Bastos, É. L. d. Albuquerque, L. S. Campos, and L. C. Wrobel. Two accelerated isogeometric boundary element method formulations: fast multipole method and hierarchical matrices method. *Lat. Am. j. solids struct.*, vol. 19, pp. e463, 2022.

[3] M. Bebendorf. Approximation of boundary element matrices. *Numer. Math.*, vol. 86, n. 4, pp. 565–589, 2000.

[4] Y. Liu. *Fast multipole boundary element method: theory and applications in engineering*. Cambridge university press, 2009.

[5] S. Börm, L. Grasedyck, and W. Hackbusch. Introduction to hierarchical matrices with applications. *Eng. Anal. Boundary Elem.*, vol. 27, n. 5, pp. 405–422, 2003.

[6] L. S. Campos, C. F. Loeffler, F. O. Netto, and dos Á. d. J. Santos. Testing the accomplishment of the radial integration method with the direct interpolation boundary element technique for solving helmholtz problems. *Engineering Analysis with Boundary Elements*, vol. 110, pp. 16–23, 2020.

[7] J. Barbosa, C. Loeffler, and L. Lara. The direct interpolation boundary element technique applied to three-dimensional scalar free vibration problems. *Engineering Analysis with Boundary Elements*, vol. 108, pp. 295–300, 2019.

[8] C. F. Loeffler and W. J. Mansur. A regularization scheme applied to the direct interpolation boundary element technique with radial basis functions for solving eigenvalue problem. *Eng. Anal. Boundary Elem.*, vol. 74, pp. 14–18, 2017.
[9] L. S. Campos and C. F. Loeffler. A new strategy for a faster matrix assembly in the boundary element method. *Comput. Math. Appl.*, vol. 174, pp. 449–453, 2024.
[10] C. A. Brebbia, J. C. F. Telles, and L. C. Wrobel. *Boundary Element Techniques*. Springer, Berlin, Germany, 1984.
[11] P. R. Johnston and D. Elliott. A sinh transformation for evaluating nearly singular boundary element integrals. *Int. J. Numer. Methods Eng.*, vol. 62, n. 4, pp. 564–578, 2005.